ASIAN JOURNAL OF PHARMACEUTICAL AND CLINICAL RESEARCH

INNOVARE ACADEMIC SCIENCES
Knowledge to Innovation

Vol 18, Issue 10, 2025

Online - 2455-3891
Print - 0974-2441

Research Article

IN SILICO CHARACTERIZATION OF IMEGLIMIN'S INTERACTION WITH INFLAMMATORY AND MITOCHONDRIAL TARGETS USING MOLECULAR DOCKING AND MOLECULAR DYNAMICS

YAZHINI P M, RAMYA S*, PARVATHAREDDY SOWMYA, KAVITHA RAMASAMY

Department of Pharmacology, Sri Ramachandra Medical College and Research Institute, SRIHER, Porur, Chennai, Tamil Nadu, India
***Corresponding author: Ramya S; Email: ramya.s@sriramachandra.edu.in**

Received: 02 July 2025, Revised and Accepted: 14 August 2025

ABSTRACT

Objectives: The objective of the study is to elucidate the molecular basis of Imeglimin's mitochondrial protective and anti-inflammatory effects through *in silico* analysis of its interactions with key mitochondrial and inflammatory regulatory proteins.

Methods: Molecular docking and 100 ns molecular dynamics simulations were performed to assess Imeglimin's binding to five key targets: AKT1, Parkin, DRP1, NLRP3, and hexokinase 2. Analyses included root mean square deviation, root mean square fluctuation, radius of gyration, principal component analysis, dynamic cross-correlation matrices, and MM/GBSA-based binding-free energy calculations.

Results: Imeglimin exhibited stable interactions with critical regulatory residues in AKT1 (kinase domain), Parkin (Ubl and RING regions), DRP1 (GTPase domain), and NLRP3 (NATCH and LRR domains). These interactions were associated with constrained conformational mobility and stabilization of inactive-like states. Hexokinase 2 showed lower binding affinity and higher flexibility. MM/GBSA analysis indicated favorable binding energetics.

Conclusion: Imeglimin acts as a multi-target modulator of mitochondrial proteins, stabilizing functionally inactive or constrained conformations without inducing structural destabilization. These findings provide a structural framework for its reported mitochondrial protective and anti-inflammatory function.

Keywords: Imeglimin, Molecular dynamics, Mitochondrial function, Parkin, DRP1, NLRP3. AKT1, Hexokinase2, *In silico* analyses.

 DOI: http://dx.doi.org/10.22159/ajpcr.2025v18i10.55851. Journal homepage: https://innovareacademics.in/journals/index.php/ajpcr

INTRODUCTION

Mitochondria, by performing a range of cellular tasks including cellular metabolism, intracellular signaling, cellular energetics, apoptosis, and immunity, are the key regulators of cellular homeostasis [1]. Mitochondrial dysfunction has emerged as a pivotal factor in the development and progression of several inflammatory [2] and metabolic disorders [3]. As a significant source of reactive oxygen species (ROS) [4], mitochondrial dysfunction leads to the generation of excessive ROS, thereby contributing to oxidative stress [3]. Mitochondrial ROS also act as signal transduction molecules driving the production of pro-inflammatory cytokines by both inflammasome-dependent and inflammasome-independent pathways [5]. Mitochondrial dysfunction has been implicated in multifactorial disorders such as rheumatoid diseases [6] such as inflammatory arthritis [7], systemic lupus erythematosus [8], osteoarthritis [9], cardiovascular diseases [10,11], neurological and neurodegenerative disorders [12-16], metabolic disorders [17-23], and neoplasms [24-26].

Primary mitochondrial diseases occur due to defects in oxidative phosphorylation (OXPHOS) [27], whereas secondary mitochondrial disorders stem from deficiencies in mitochondrial quality control, biosynthesis, metabolism, and dynamics [28]. Targeting mitochondrial dysfunction is essential as it represents a therapeutic gap in the management of various multifactorial disorders. Recent advancements in pharmacological research have focused on modulating mitochondrial biogenesis [29-31], bioenergetics, and metabolism to improve disease outcomes [32-36].

Imeglimin, a next-generation anti-diabetic drug, first in the new class "glimins" [37], represents a promising candidate in this context, as studies indicate that it can effectively modulate mitochondrial function. Imeglimin distinguishes itself from other classes of anti-diabetic drugs through its dual mechanism of action, which involves both enhancing secretion through glucose-stimulated insulin secretion and restoring β-cell function [38].

Imeglimin has been shown to modulate OXPHOS activity by exerting a partial inhibition of Complex 1 while simultaneously restoring Complex 3 function, resulting in a metabolic shift, redirecting the substrate flow through Complex 2 (succinate pathway). In addition, Imeglimin prevents the reverse electron transfer through Complex 1 [39], a key pathway involved in excessive mitochondrial ROS production. Beyond regulating mitochondrial respiration, imeglimin has been observed to reduce ROS production and NADPH oxidase subunit expression, thereby mitigating oxidative stress. Moreover, it also enhances mitochondrial biogenesis through a PGC1α-independent mechanism and improves mitochondrial bioenergetics by increasing ATP production [38,39]. Imeglimin has also been found to inhibit the opening of mitochondrial membrane permeability transition pore, which is a critical event in apoptotic cell death, thereby conferring an anti-apoptotic effect [39]. Furthermore, studies also indicate that Imeglimin treatment leads to the downregulation of inflammatory markers, suggesting its potential to modulate inflammation [40-43].

This study employs computational simulations to characterize imeglimin's interaction with key mitochondrial and inflammation-associated proteins, protein kinase B (AKT1), dynamin-related protein 1 (DRP1), Parkin with intact Ubl domain, and Hexokinase 2. By elucidating the binding interaction of Imeglimin with these targets, this study aims to uncover potential mechanisms by which Imeglimin modulates mitochondrial and inflammatory pathways.

METHODS

For the molecular docking study, the three-dimensional structure of Imeglimin was retrieved from the PubChem database. The three-dimensional protein structures of AKT1 (PBD ID: 7NH5) [44], DRP1 [45], Parkin (UblR0RBR) (PDB ID: 5C1Z) [46], NLRP3 (PDB ID: 7ALV) [47,48], and Hexokinase2 (PDB ID: 2NZT) [48] were obtained from the PDB database. AutuDockTools1.5.7 and Autodock4.0 software packages were used for preparing and docking the proteins and ligands. The binding affinity of the target proteins was assessed. Among the analyzed proteins, AKT1, DRP1, Hexokinase 2, Parkin (UblR0RBR), and NLRP3 demonstrated favorable binding energies, indicative of strong ligand–protein interaction. Based on these results, these proteins were selected for further molecular dynamics simulation study.

The topology and coordinate parameters for the molecular systems were generated using the AMBERff19SB force field [49] within the LEAP module of the AmberTools22 package [50]. Molecular dynamics (MD) simulations spanning 100 ns were performed using the OPENMM software package [51]. To simulate a biologically relevant environment, the protein–ligand complex structures were solvated in a TIP3P explicit water model with a 10 Å buffer around each side. Neutralization was achieved by adding Na^+/Cl^- ions. The system was subsequently minimized using the steepest descent and conjugate gradient algorithms for 10,000 steps to eliminate steric clashes and optimize the system's initial conformation. Following minimization, the system underwent equilibration for 2 ns under NPT ensemble conditions at a temperature of 298 K and 1 atm pressure. Subsequently, 100 ns production MD simulations were conducted for Imeglimin in complex with AKT1, DRP1, Hexokinase, Parkin (UblR0RBR), and NLRP3 employing an NPT ensemble (isothermal–isobaric conditions) with a constant temperature (300 K) and pressure (1 bar) using a 10fs time step. To assess the structural stability and conformational dynamics of the protein–ligand complexes, root mean square deviation (RMSD) and root mean square fluctuation (RMSF) analyses were performed. In addition, principal component analysis (PCA) and dynamic cross-correlation matrix (DCCM) plots were generated using CPPTRAJ [52] to elucidate the global motion and correlated atomic fluctuations within the complexes. To investigate intermolecular interactions, hydrogen bonding and hydrophobic interactions were analyzed using PyMOL (The PyMOL Molecular Graphics System, Version 2.0, Schrodinger LLC) and Discovery Studio Visualizer (BIOVIA, SanDiego, USA). The binding-free energy (MM/GBSA) calculations were performed from the 100 ns MD simulation trajectories using the MMPBSA.py routine available in AmberaTools22.

RESULTS

Imeglimin demonstrated strong binding with DRP1 (−27.1 kcal/mol) and Parkin (−26.7 kcal/mol), moderate binding with AKT1 (−18.3 kcal/mol) and NLRP3 (−12.9 kcal/mol), and weak binding with Hexokinase 2 (−6.1 kcal/mol) during 100 ns molecular dynamic simulation highlighting its varying affinities across target proteins (Table 1). Also, the intermolecular interactions between Imeglimin and amino acids of the proteins, AKT1, Parkin, DRP1, Hexokinase, and NLRP3 during docking and 100 ns MD simulation can be found in Table 2.

Table 1: MMGBSA binding-free energy of Imeglimin with AKT1, Drp1, Hexokinase, NLRP3, and Parkin enzyme complexes (in kcal/mol)

Target	E VdW	E EL	E GB	E SURF	G gas	G solv	G Bind
AKT1	−21.7	−18.7	24.5	−2.5	−40.4	22.1	−18.3
Parkin	−13.0	−139.1	128.0	−2.7	−152.0	125.3	−26.7
DRP1	−16.7	−52.5	45.3	−3.2	−69.2	42.1	−27.1
Hexokinase 2	−17.4	24.4	−10.3	−2.8	6.9	−13.1	−6.1
NLRP3	−15.87	−126.0	131.5	−2.4	−141.9	129.0	−12.9

E VdW: Van der Waals Energy, E_EL: Electrostatic energy, EGB: Generalized born electrostatic energy, E SURF: Nonpolar solvation energy, G gas: Gas phase energy, G Solv: Solvation-free energy, G Bind: Binding-free energy

Imeglimin and AKT1

Molecular docking revealed initial hydrogen bonding with residues Tyr229, Glu234, Phe236, Glu278, Leu280, Thr291, Phe293 and hydrophobic interactions with Tyr229 and Phe293, suggesting binding near the activation loop [53]. MD simulations refined the interaction, revealing persistent hydrogen bonds with Glu278and Thr291 and new hydrogen interactions at Tyr272 and Asn279 (Fig. 1). Loss of hydrophobic interactions was observed during MD simulation. Fig. 2a shows the RMSD of the Imeglimin-AKT1 complex. The protein backbone deviation during the simulation ranged from 0.0Å to 2.76 Å. The RMSD values initially fluctuated but stabilized after approximately 10 ns, and the values stabilized with an average of 2.04Å. Fig. 2b shows the RMSF of Imeglimin-AKT1. Observed RMSF values of the interaction. RMSF values of the binding residues are Glu278: 0.470795Å, Asn279: 0.443976Å, Thr291: 0.501664Å, and Tyr272: 0.480740Å. Fig. 2e shows the radius of gyration (Rg) of Imeglimin-AKT1. The Rg analysis reveals an average value of 21.57Å with a narrow fluctuation range (21.33 Å - 21.76 Å). In the Imeglimin-AKT1 complex PCA graph (Fig. 2d), the eigenvalues were plotted against the eigenvector indices. Dominant movements were seen in the first five eigenvectors, which accounted for 16.1%–51.2% of the variation overall. The first three principal components (PC1, PC2, and PC3) accounted for 16.1%, 9.9%, and 5.89% of the variance, respectively, collectively explaining over 31.89% of the system's essential dynamics. PC1 captured large-scale domain shifts while PC2 and PC3 highlighted localized motions around the binding site. The DCCM map (Fig. 2c) of the AKT1-Imeglimin complex exhibits strongly correlated motion patterns within the kinase domain, and no significant anti-correlations were observed between the domains of AKT1. The binding energetics (Table 2) calculated revealed a favorable binding-free energy of 18.3 kcal/mol. This stability was primarily driven by Van der Waals (−21.7 kcal/mol) and electrostatic (−18.7 kcal/mol) interactions. While a solvation penalty (+22.1 kcal/mol) was observed, it was outweighed by favorable gas-phase interactions (−40.4 kcal/mol).

Imeglimin-Parkin

Molecular docking analysis revealed initial hydrogen bond interactions between Imeglimin and Gly47, Lys48, Glu49, Thr180, Tyr331, with a strong hydrophobic interaction at Lys48. These residues are located in the Ubl, RING0, RING1, IBR, and RING2 domains of Parkin. MD simulations refined these interactions, showing persistent hydrogen bonding with Thr180& Tyr331 and new hydrogen bonds with Cys181, Thr182, Asp334, Arg336 (Fig. 3). Hydrophobic interactions with Lys48 were slightly weakened during the MD trajectory. Fig. 4a represents the RMSD of Imeglimin–Parkin complex. The protein backbone deviation exhibited fluctuations during the first 5 ns. Beyond this phase, the value stabilized with an average value of 3.7Å throughout the simulation. Transient sporadic peaks reaching up to 5.92 Å were observed. Fig. 4b shows the Rg of Imeglimin-Parkin. The values ranged from 25.12 Å to 26.47 Å, with an average of about 25.96 Å with minimal fluctuations. Stabilization occurred at about 1.6 ns of the simulation. Fig. 4c represents the RMSF of Imeglimin–Parkin interaction. The RMSF values of interacting residues were observes as Thr180: 1.20788 Å, Cys181: 1.4095 Å, Thr182:1.4970 Å, Tyr331: 1.7556 Å, Asp334: 1.7560 Å, Arg336: 1.9031 Å & Lys48: 1.1087 Å. In Imeglimin-Parkin PCA graph (Fig. 4d), the eigenvalues were plotted against the eigenvector indices. It illustrates the dominant structural motions captured in the first PCs. PC1 (31.12%) represents large-scale domain movements primarily in RING1 and RING2, while PC2 (18.87%) and PC3 (9.1%) depict localized flexibility in RING0 and the binding pocket. The complex remained within a restricted conformational space. Binding-free energy (Table 2) indicates that Imeglimin binds Parkin with high affinity (−26.7 kcal/mol) predominantly through electrostatic interactions (−139.1 kcal/mol) with additional Van der Waals stabilization (−13.0 kcal/mol).

Imeglimin-DRP1

Molecular docking analysis revealed initial hydrogen bond interactions between Imeglimin Thr215, Lys216, Asp218, Leu219, Asn246, Arg247, and Ser248 with a strong hydrophobic interaction at Lys216 of DRP1. These residues are located in the GTPase domain, crucial for its enzymatic activity. MD simulations refined these interactions,

showing persistent hydrogen bonding with Asn246 and Ser248, while new hydrogen bonds emerged with Asp251, Ser261, and Asp264. Hydrophobic interactions shifted from Lys216 to Asp264 (Fig. 5). Fig. 6a shows RMSD of Imeglimin-DRP1 complex. The protein backbone deviation exhibited fluctuations during the initial 20 ns. Beyond this phase, the value stabilized with an average of about 2 Å. Fig. 6b shows the radius of gyration Rg of Imeglimin-DRP1 complex. The values ranged from 22.0 Å to 22.6 Å, with an average of about 22.31 Å with minimal fluctuations. Fig. 6c represents the RMSF of Imeglimin-DRP1 complex. The RMSF values of interacting residues were observed as Asn246: 0.7943 Å, Ser248: 1.1575 Å, Asp251: 1.9628 Å, Asp264: 0.8221 Å. The DCCM map (Fig. 6e) of Imeglimin-DRP1 shows coordinated motions within the GTPase domain. DCCM map suggests ligand-induced conformational restrictions that may impair DRP1 flexibility. In the Imeglimin-DRP1 PCA graph (Fig. 6d), the eigenvalues were plotted against eigenvector indices. It illustrates the dominant structural motions captured in the first PCs. PC2 (31.11%) represents large-scale domain movements, while PC1 (27.68%) and PC3 (8.08%). The PC1-PC2 projection showed a wide conformational spread. The Scree plot shows a rapid decline in eigenvalues after PC3. MM/GBSA analysis (Table 2) estimates the binding-free energy at −27.1 kcal/mol, indicating high affinity with electrostatic interactions (−52.5 kcal/mol) being the predominant contributor, while Van der Waals interaction (−16.7 kcal/mol) stabilized the complex.

Table 2: Intermolecular interactions between Imeglimin and amino acids of different proteins (AKT1, Parkin, DRP1, Hexokinase, and NLRP3) during docking and 100 ns MD simulation

Target protein	Interacting amino acid residues (Distance Å)			
	Docking		Dynamics	
	Hydrogen bond	Hydrophobic interaction	Hydrogen bond	Hydrophobic interaction
AKT1	Tyr229 (2.2), Glu234 (2.1), Phe236 (3.0), Glu278 (2.1), Leu280 (3.4), Thr291 (3.0), Phe293 (2.3)	Tyr229 (3.3), Phe293 (3.4)	Tyr272 (2.5), Glu278 (2.6), Asn279 (3.3), Thr291 (2.0)	Nil
Parkin	Gly47 (2.4), Lys48 (2.4), Glu49 (2.6), Thr180 (2.3), Tyr331 (2.2)	Lys48 (3.6)	Thr180 (3.3), Cys181 (2.8), Thr182 (2.7), Tyr331 (3.2), Asp334 (3.4), Arg336 (3.4)	Lys48 (3.9)
DRP1	Thr215 (3.5), Lys216 (2.7), Asp218 (2.0), Leu219 (3.0), Asn246 (1.9), Arg247 (3.3), Ser248 (2.6)	Lys216 (3.4)	Asn246 (3.0), Ser248 (3.4), Asp251 (1.9), Ser261 (3.1), Asp264 (1.8)	Asp264 (3.8)
Hexokinase 2	Gly86 (2.9), Gly87 (3.1), Thr88 (2.8), Asn89 (2.9), Phe90 (3.0), Tyr112 (3.0), Ile114 (1.9), Met119 (3.2)	Ile111 (4.0)	Lys337 (3.1), Ser340 (3.1), Ser415 (2.8), Val416 (2.8), Lys419 (3.1)	Thr232 (3.9)
NLRP3	Arg351 (2.9), Val353 (3.5), Arg578 (2.1), Gln624 (1.8), Ser626 (2.7), Glu629 (3.0), Asp662 (3.0)	Leu628 (4.6), Tyr632 (4.1)	Ala228 (3.2), Ile574 (2.7), Arg578 (3.2), Glu629 (3.0), Tyr632 (3.1)	Tyr632 (3.4)

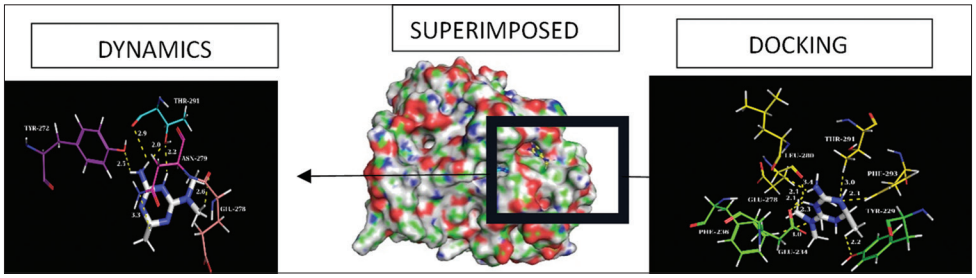

Fig. 1: Interaction of Imeglimin with AKT1 at the end of 100 ns MD simulation and during docking

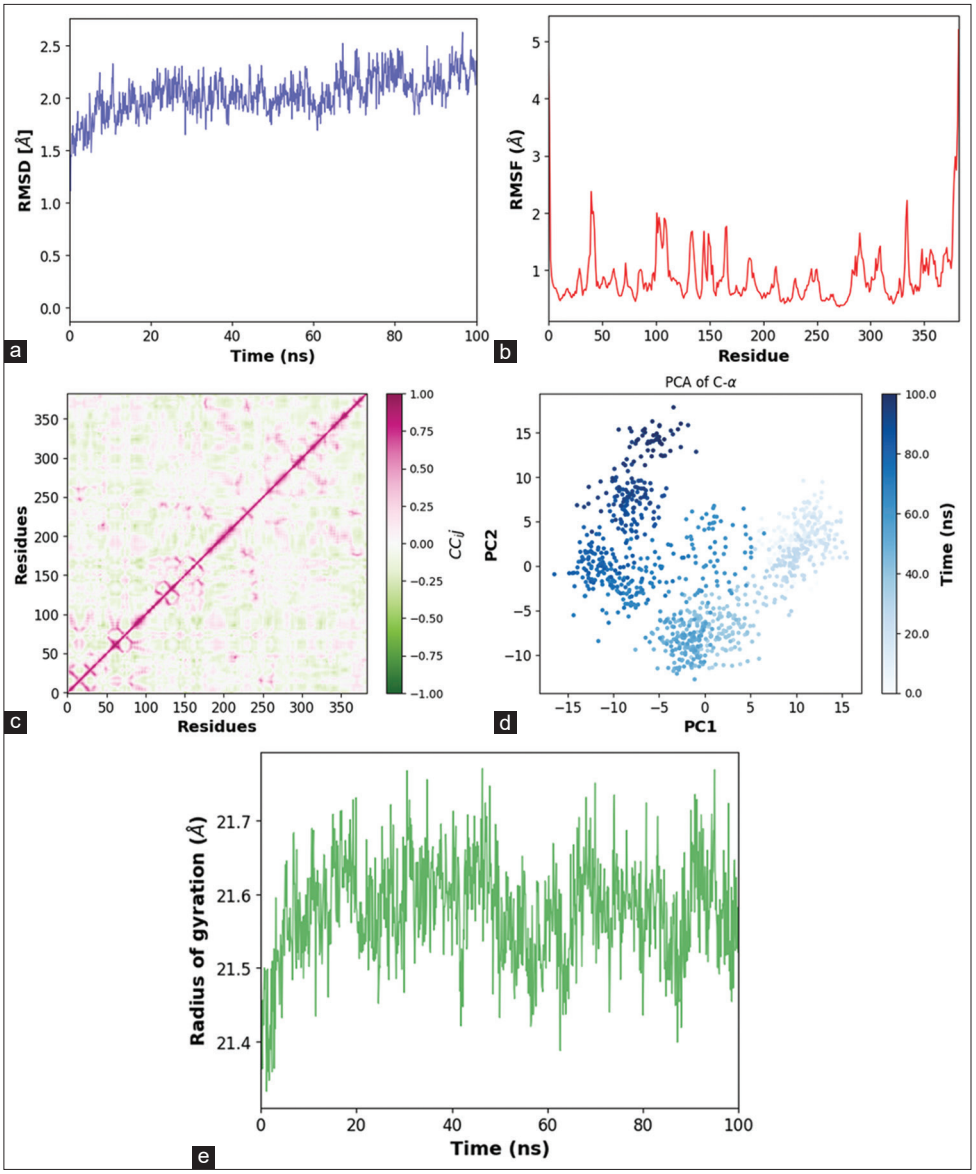

Fig. 2: (a) Root mean square deviation (b) root mean square fluctuation (c) dynamic cross-correlation matrix (d) principal component analysis (e) Radius of gyration plots of Imeglimin/AKT1 during MD simulation

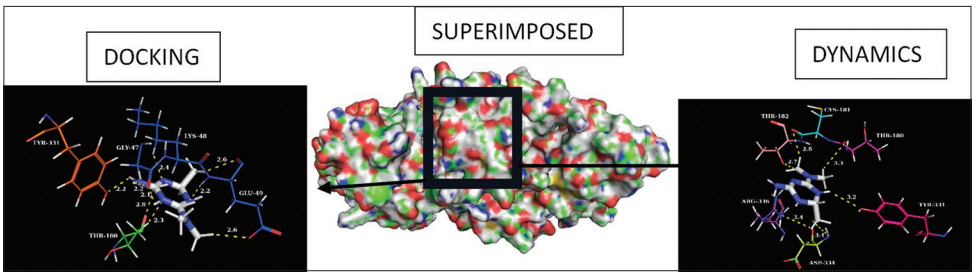

Fig. 3: Interaction of Imeglimin with Parkin during docking at the end of a 100 ns MD simulation

Imeglimin–Hexokinase 2

Molecular docking analysis revealed initial hydrogen bond interactions between Imeglimin and Hexokinase 2 at Gly86, Gly87, Thr88, Asn89, Phe90, Tyr112, Ile114, and Met119, with a strong hydrophobic interaction at Ile111. MD simulations refined these interactions, showing the formation of new hydrogen bonds with Lys337, Ser340, Ser415, Val416, and Lys419, while initial interactions observed in docking were lost. Hydrophobic interactions were observed at Thr232, suggesting that Imeglimin underwent binding site migration during the simulation (Fig. 7). Fig. 8a represents the RMSD of the Imeglimin–Hexokinase2 complex. The protein backbone fluctuations spanned 1.2–4.2Å over 100 ns simulation. No specific stabilization phase was observed. The Rg values fluctuated between 38.39 Å and 40.62 Å with the majority of the values lying in the range of 39.52Å to 39.97 Å Fig. 8b. RMSF (Fig. 8c) represents the RMSF of Imeglimin–Hexokinase2. The RMSF values of key interacting residues were Lys337: 1.4132 Å, Ser340: 1.3428 Å, Ser415: 0.9450 Å, Val416: 0.8921 Å, and Lys419: 1.2570 Å. The PCA analysis (Fig. 8d)

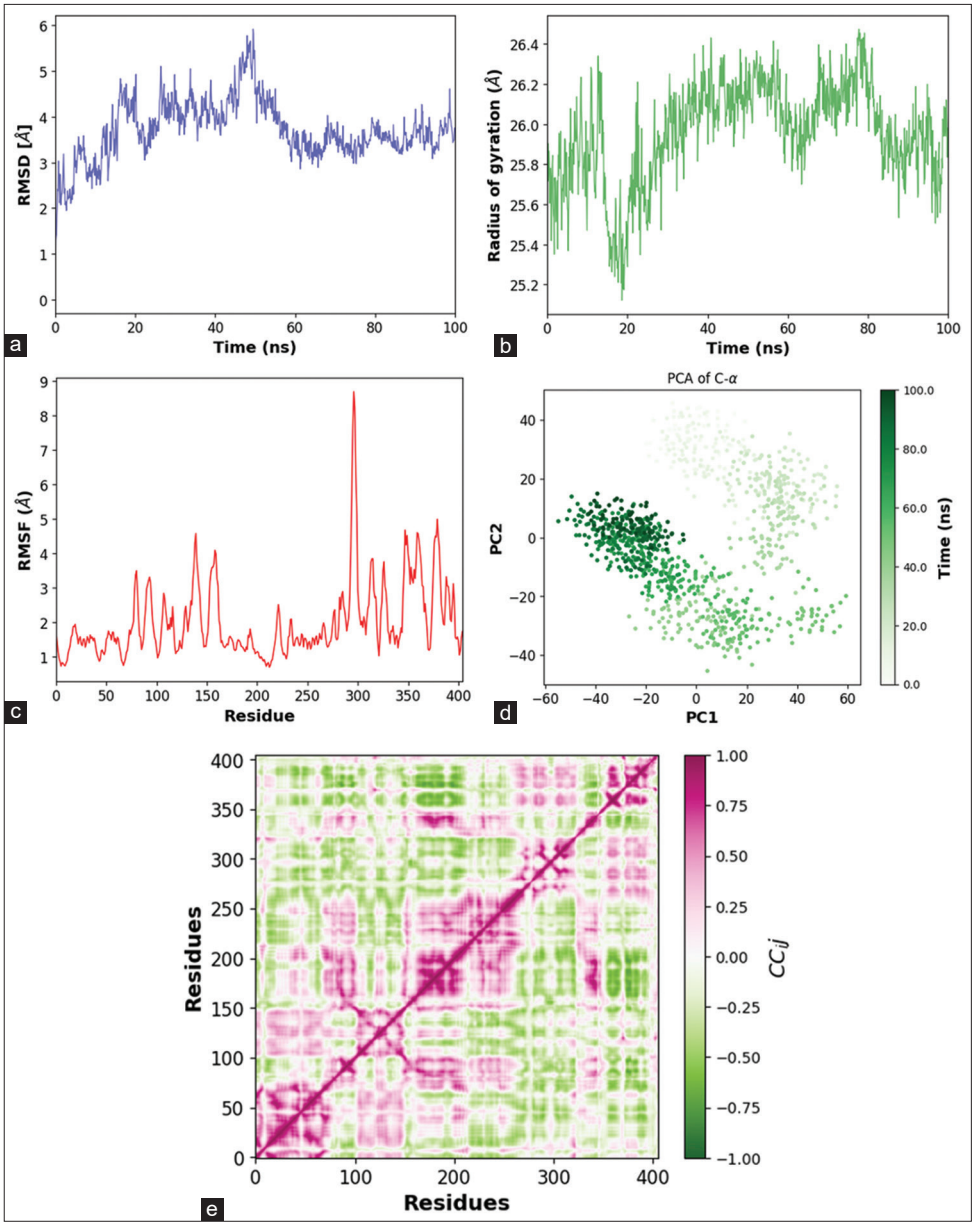

Fig. 4: (a) Root mean square deviation (b) Radius of gyration (c) root mean square fluctuation (d) principal component analysis (e) dynamic cross-correlation matrix plots of Imeglimin/Parkin during MD simulation

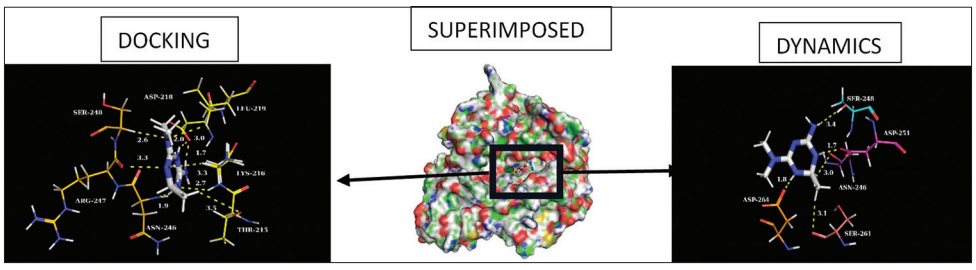

Fig. 5: Interaction of Imeglimin with DRP1 during docking at the end of a 100 ns MD simulation

revealed that the first PCs capture 68.75% of the total variance with PC1 (38.05%), PC2 (22.27%), and PC3 (8.43%). The scree plot confirms that PC1 and PC2 dominate the conformational landscape while the higher-order PCs contribute less. A steep drop is observed after PC2, with PC3 adding minor fluctuations. The DCCM analysis (Fig. 8e) reveals both correlated and anti-correlated motions within Hexokinase2-Imeglimin complex. Strongly correlated motions were observed within localized regions, while anti-correlated motions were observed between distant regions. Table 2 presents the MM/GBSA binding-free energy calculations, indicating that Imeglimin binds Hexokinase 2 with low affinity (−6.1 kcal/mol). Electrostatic interactions were destabilizing (+24.4 kcal/mol) while Van der Waals interactions (−17.4 kcal/mol) and solvation effects (−1.03 kcal/mol) provided some stabilization.

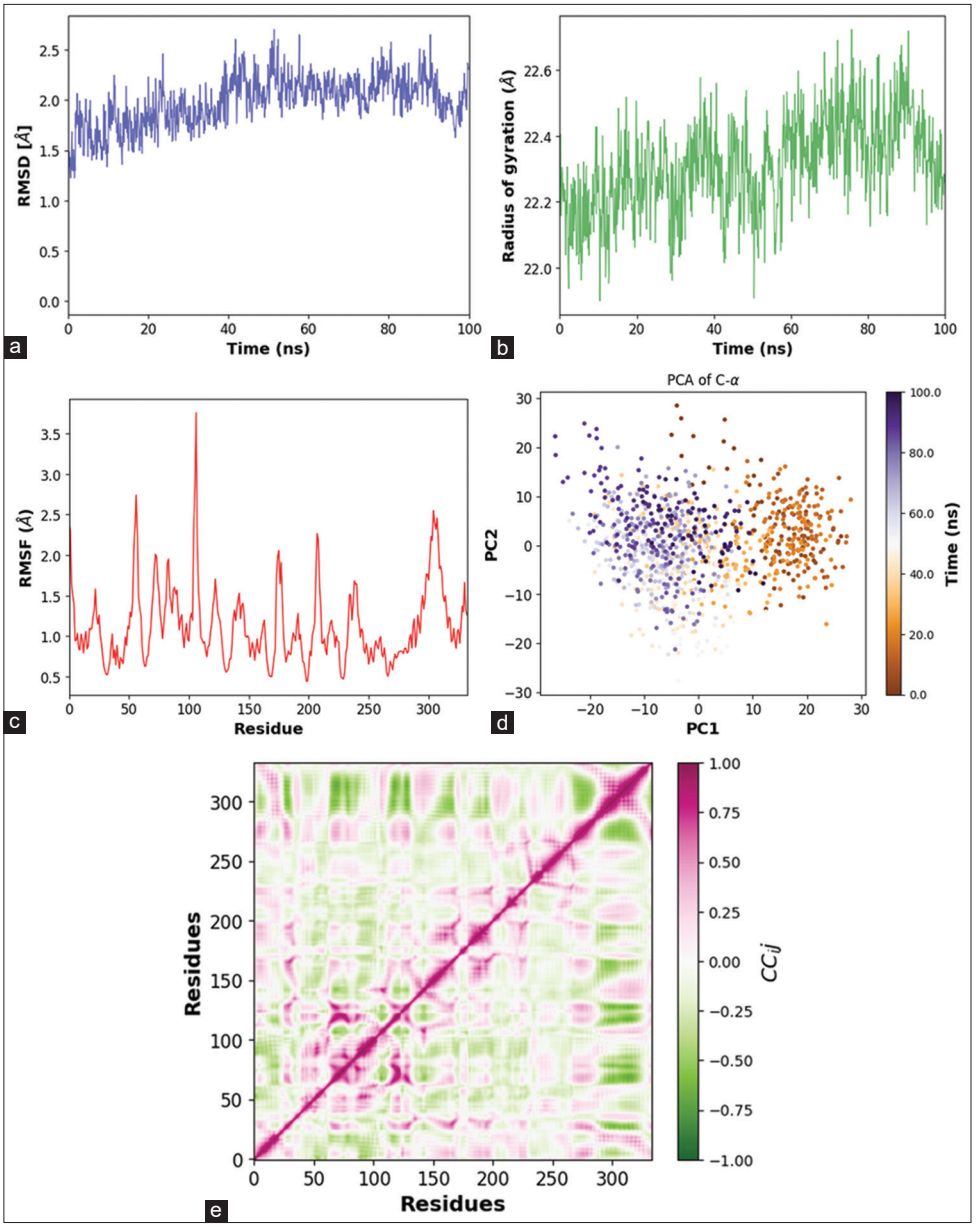

Fig. 6: (a) Root mean square deviation (b) Radius of gyration (c) root mean square fluctuation (d) principal component analysis (e) dynamic cross-correlation matrix plots of Imeglimin/DRP1 during MD simulation

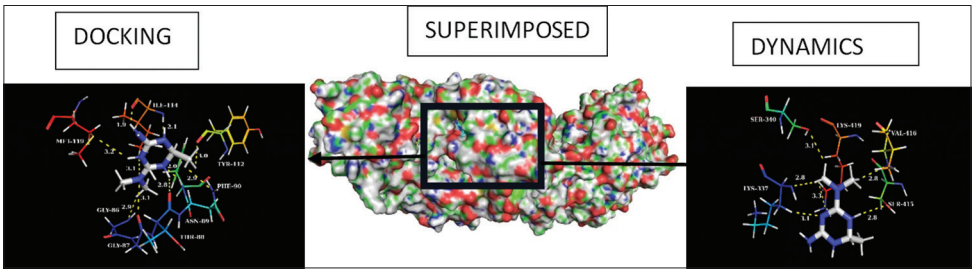

Fig. 7: Interaction of Imeglimin with Hexokinase 2 during docking at the end of a 100 ns MD simulation

Imeglimin-NLRP3

Molecular docking analysis revealed initial hydrogen bond interactions between Imeglimin and Arg351, Val353, Arg578, Gln624, Ser626, Glu629, and Asp662, with hydrophobic interactions at Leu628 and Tyr632. MD simulation refined these interactions, showing persistent hydrogen bonding with Arg578 and Glu629 while introducing new hydrogen bonds with Ala228, Ile574, and Tyr632. Hydrophobic interaction with Tyr632 emerged during the trajectory while the initial hydrophobic interactions weakened (Fig. 9). The residues involved in hydrogen bonding are located in the NATCH and LRR domains of NLRP3, which are critical for ATP binding and inflammasome activation. Fig. 10a represents the RMSD of Imeglimin-NLRP3 complex.

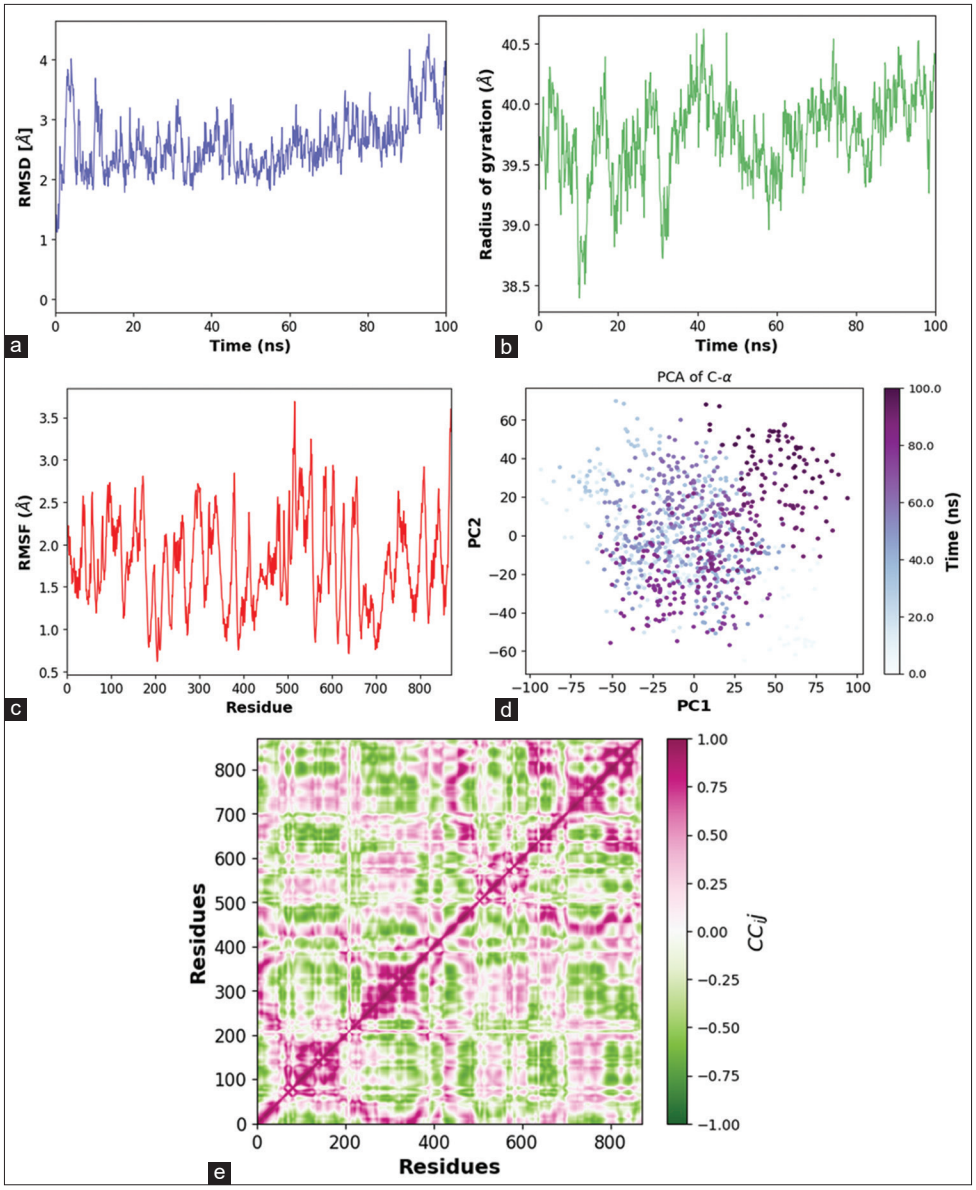

Fig. 8: (a) Root mean square deviation (b) Radius of gyration (c) root mean square fluctuation (d) principal component analysis (e) dynamic cross-correlation matrix plots of Imeglimin/Hexokinase 2 during MD simulation

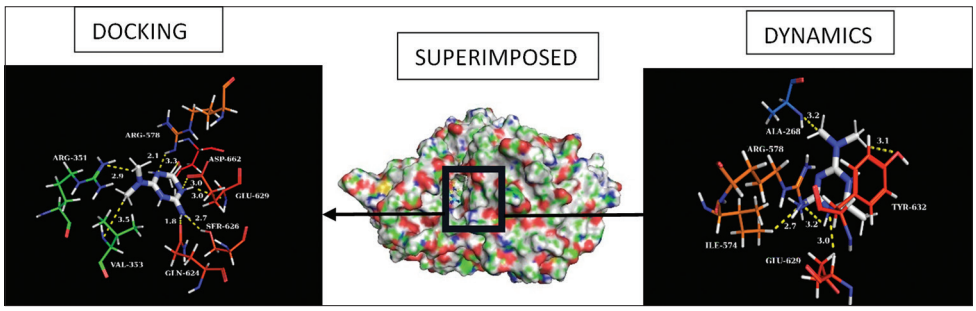

Fig. 9: Interaction of Imeglimin with NLRP3 during docking at the end of a 100 ns MD simulation

The protein backbone deviation exhibited fluctuations in the initial 5 ns post which minor fluctuations were observed until 20 ns. Beyond 20 ns, the values stabilized with an average of 1.2–1.3 Å throughout the simulation. Transient peaks reaching up to 3.0 Å were observed, but no significant unfolding was observed. Fig. 10b shows the Rg of Imeglimin–NLRP3 complex. The values range from 22.8 Å to 23.4 Å, indicating the compactness of the complex. Fig. 10b represents the Rg of the complex that remained compact throughout the simulation. Fig. 10c represents RMSF of Imeglimin–NLRP3 interaction. The RMSF values of the interacting residues were observed as Ala228: 0.7884 Å, Ile574: 0.7688 Å, Arg578: 0.4789 Å, Glu629: 0.8716 Å, Tyr632: 0.6108 Å. In the Imeglimin-NLRP3 PCA graph (Fig. 10d), the eigenvalues were

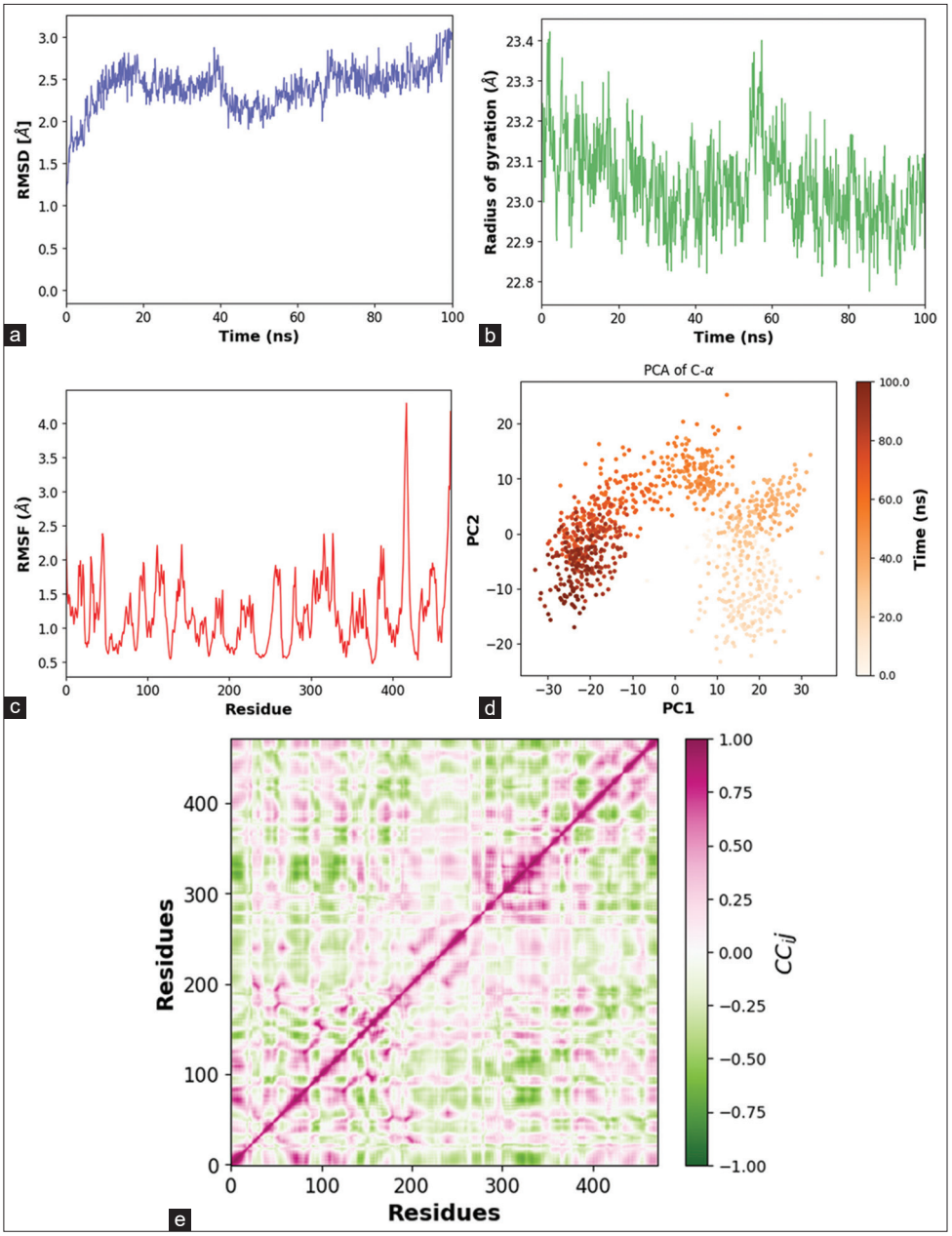

Fig. 10: (a) Root mean square deviation (b) Radius of gyration (c) root mean square fluctuation (d) principal component analysis (e) dynamic cross-correlation matrix plots of Imeglimin/NLRP3 during MD simulation

plotted against eigenvector indices to illustrate dominant motions captured during the simulation. The first PCs capture 54.69% of the total variance with PC1 (39.4%), PC2 (9.14%), and PC3 (6.15%). A steep decline in eigenvalues is observed after PC3. The DCCM (Fig. 10e) reveals positive correlations in the NATCH domain, while anti-correlated regions were observed in LRR domain. Table 2 presents the MM/GBSA binding-free energy calculations, indicating that Imeglimin binds NLRP3 with moderate affinity (−12.9 kcal/mol). Electrostatic interactions were dominant (−126.0 kcal/mol), while Van der Waals interactions (−15.87 kcal/mol). A desolvation penalty of +131.5 kcal/mol and solvation energy of −2.4 kcal/mol was observed.

DISCUSSION

Imeglimin-AKT1

AKT1 is an AGC kinase [54] that regulates many processes such as cell survival, metabolism, growth, and proliferation [55-59]. AKT1 activation is a multistep process that necessitates phosphorylation of two key residues, Thr308 in the activation loop of the kinase domain by PDK1, followed by Ser473 in the hydrophobic motif of the C-terminal regulatory domain by mTORC2. AKT1 exists in an auto-inhibited state in the cytoplasm. The PH domain of akt1 is found to interact with the kinase domain, preventing spontaneous activation by PIP3. Upon the activation of PIP3 pathway, PH domain binds with PIP3, and its interaction with the kinase domain is lost, which undergoes conformational changes that expose Thr308, making it accessible to PDK1 phosphorylation. The interdomain flexibility of AKT1 increases transitioning to a more open conformation of akt1, enabling Ser473 phosphorylation by mTORC2, leading to complete activation. For termination of the signaling, AKT1transitions to a closed conformation, making it accessible for PP2A and PHLPP to dephosphorylate AKT1 [60-62].

Co-Crystal Structure of Akt1 in Complex with Covalent–Allosteric AKT1 Inhibitor 6 (PDB ID:7NH5) was taken up for the computational study. Molecular docking and dynamic simulation studies revealed

that Imeglimin forms persistent hydrogen bonding at Glu278, Thr291, Asn279, and Tyr272. Although these residues are not the sites of phosphorylation of AKT1, they are located in the kinase domain [60]. The low RMSF values of the binding residues indicate that Imeglimin binding reduces the flexibility of the kinase domain and stabilizes AKT1 in a certain conformation. The stable RMSD values of the alpha carbon atom of AKT1 during simulation indicate that Imeglimin does not induce large-scale conformational changes in AKT1. In addition, the stable Rg values observed during the study indicate that the Imeglimin-AKT1 complex maintains a compact structure. PCA analysis suggested that the complex remained within a restricted conformational cluster, indicating that AKT1 remains locked in a specific structural state. In DCCM analysis, strongly correlated motion within the kinase domain suggests Imeglimin reinforces an internally stable conformation, and the limited anti-correlated motion between the loops and the rest of the kinase domain indicates that the activation loop remains structurally constrained. Free energy calculations showed that Imeglimin binds stably to AKT1 with strong contributions from Van der Waals and electrostatic interactions. These findings collectively indicate that Imeglimin stabilizes AKT1 in a structured conformation, restricting its large-scale motion. Since AKT1 activation requires significant conformational changes [63] in the activation loop, this suggests that Imeglimin does not facilitate direct activation but may influence phosphorylation retention or substrate interactions.

AKT1 plays a critical role in mitochondrial biogenesis, metabolism and bioenergetics, oxidative stress regulation, and mitophagy [64-66]. It is also a key regulator of the inflammatory signaling pathway [58,67,68], particularly through NF-Kb and mTORC1 activation. By stabilizing AKT1 in a constrained conformation, Imeglimin may influence its ability to mediate inflammatory responses. Given Imeglimin's established mitochondrial protective [39,41,69] and anti-inflammatory effects [42,43], this interaction provides a structural basis for potential mechanisms of action through AKT1 modulation.

Imeglimin-Parkin

Parkin, an E3 ubiquitin ligase, exists in an auto-inhibits state and requires phospho-ubiquitin binding and phosphorylation of its N-terminal ubiquitin-like (Ubl) domain by PINK1 for full activation. In its inactive state, the Ubl domain interacts with catalytic domains that prevent activation. Activation involves conformational changes that expose the catalytic RING2 domain, allowing ubiquitination of substrate [70-73].

Parkin (UblR0RBR) (PDB ID: 5C1Z) was used for computational analysis. Molecular docking and MD simulations demonstrated that Imeglimin forms stable hydrogen bonds with Thr180, Tyr331, Cys181, Thr182, Asp334, and Arg336 and hydrophobic interaction with Lys48. Lys48, located in the Ubl domain, is the most stable residue (RMSF=1.1087 Å) suggesting that it might play an anchoring role in binding. Moderate flexibility was observed in Thr180 (RMSF=1.20788 Å), Cys181 (RMSF: 1.4095 Å), Thr182 (RMSF: 1.4970 Å), which are located in the RING0 domain. These residues are known to play a role in Parkin's auto-inhibitory state. The observed increase in flexibility in these regions may indicate a partial destabilization of the inhibitory interactions. Tyr331 located in RING1 domain exhibited higher fluctuation in the imeglimin-bound complex, suggesting increased flexibility at the key structural interface. Since RING1 domains play a role in recruiting Ubiquitin-conjugating enzymes [74], this observed flexibility may indicate a shift in inter-domain dynamics. Higher fluctuation suggests increased flexibility at Asp334 of the IBR domain, which suggests that Imeglimin binding disrupts rigid domain interactions. Arg336 in the RING2 domain, located near the catalytic site, exhibited the highest fluctuation, indicating binding-induced structural adjustments. The observed fluctuations, especially in the residues in RING2 and IBR domains, mirror trends observed in studies of Parkin activating variants, where regulatory flexibility was associated with increased functional potential. Computational analysis study of Parkin with activating mutations [75] reported RMSF values exceeding 4Å in critical domains, similar to localized fluctuations observed in Imeglimin-bound complex, suggesting that Imeglimin induces localized flexibility in regions critical for Parkin's function, potentially facilitating a transition from auto-inhibited state to a primed state. The RMSD values of the Parkin backbone stabilize between 5Å and 6Å, whereas those of activating mutations exhibit broader RMSD variations [75]. The stable RMSD (3.5–4 Å) of the Imeglimin-bound Parkin backbone suggests that Imeglimin does not cause significant destabilization but induces local flexibility in key regulatory domains. Similarly, Rg values indicate that Parkin remains compact with only minor expansion (~26.4 Å), indicating priming rather than activation. PCA analysis revealed that Imeglimin-bound Parkin remains within a constrained conformational space, suggesting that while Imeglimin does not induce large-scale activation, it may weaken the auto-inhibitory interactions. DCCM analysis revealed strong positive correlations in the Ubl and IBR domains, indicating stabilized intra-domain interactions, while negative correlations between Ubl and RING domains suggest inter-domain flexibility. These anti-correlated motions align with RMSD and RMSF findings, suggesting that Imeglimin stabilizes Parkin's binding interfaces while promoting domain flexibility essential for functional transitions, potentially weakening the auto-inhibitory interactions while priming Parkin for activation [76]. Binding-free energy calculations indicate that Imeglimin binds Parkin with high affinity predominantly through electrostatic interactions with additional Van der Waals stabilization. Parkin activation requires large-scale conformational changes. The results indicate that Imeglimin does not induce these large-scale motions but rather promotes domain flexibility in a controlled manner, suggesting a possible priming [75-77] mechanism rather than direct activation. Thus, Imeglimin could allosterically modulate Parkin. Given the crucial role of Parkin in mitophagy and mitochondrial homeostasis [78-83] and that Imeglimin is known for its Mitochondrial protective effects [39-42,69,84], this interaction provides a potential structural basis for Imeglimin's role in mitochondrial function.

Imeglimin-DRP1

Dynamin-related protein 1 is a key GTPase regulating mitochondrial fission [85]. It exists in a dynamic equilibrium between the cytosol and mitochondria. In its inactive state, drp1 exists in the cytosol and undergoes oligomerization and conformation changes upon recruitment to mitochondria. The GTPase domain of drp1 consists of sub-domains, the nucleotide binding pocket (G1-G5) motifs responsible for GTP recognition, the Switch I and Switch II regions that regulate GTP hydrolysis, the Bundle Signaling Element transmitting conformational changes, and the dimerization interface essential for oligomerization and function activation [86].

The GTPase domain-containing construct of drp1 (PDB ID: 3W6P) was used for computational analysis. Molecular docking and MD simulations revealed that Imeglimin binds within the GTPase domain. It forms persistent hydrogen bonds with Asn246, Ser248, Asp251, Ser261, and Asp264 and a hydrophobic interaction with Asp264. Asn246 is located in the G5 motif of GTPase domain, and it stabilizes the guanine base of GTP, thereby playing a key role in nucleotide recognition [86]. Imeglimin binding at Asn246 might interfere with GTP binding. Other residues involved in bonding are not directly involved in nucleotide binding but are located within the catalytic domain, suggesting that Imeglimin could modulate drp1's enzymatic activity. The low RMSF values of Asn246 and Asp264 suggest that Imeglimin stabilizes specific regions of the GTPase domain, while Ser248 and Asp251 exhibit comparatively moderate flexibility, which indicates localized conformational adaptability. Imeglimin stabilizes Asn246 with low RMSF value (0.79Å), reducing its flexibility, suggesting that Imeglimin could influence nucleotide recognition, thereby restricting drp1's activation dynamics. The RMSD trajectory (1.5–2.5 Å) of Imeglimin-bound drp1 complex suggests that ligand binding does not induce large-scale conformational changes. Similarly, Rg values indicate that the complex remains compact, suggesting Imeglimin stabilizes drp1 within a constrained conformational space. PCA analyses revealed that the first two PCs (PC1 and PC2) accounted for 58.79% of the total variance, which indicates

that Imeglimin binding significantly influences drp1's dominant motion patterns. The plot reveals a transition from a broader conformational space to a more restricted cluster over time. This suggests that Imeglimin stabilizes drp1 within a defined structural state, thereby limiting drp1's ability to undergo large-scale conformational changes required for its activation cycle. DCCM analysis revealed strongly correlated motions within the GTPase domain, indicating that Imeglimin reinforces a stable conformation. Observed anti-correlated motion between distant regions suggests potential hinge-like movements, which may restrict large-scale movements essential for activation. The observed structural constraints suggest that Imeglimin does not promote drp1 activation but modulates its flexibility, possibly limiting excessive mitochondrial fragmentation. Binding-free energy calculations confirm strong and stable interactions between Imeglimin and drp1, with electrostatic interaction and van der Waals forces contributing significantly to binding stability. These findings collectively suggest that Imeglimin stabilizes drp1 in a structure conformation, restricting the large-scale changes necessary for full activation. Drp1 is a crucial regulator of mitochondrial quality control [87,88]. drp1 inhibition is being studied for various conditions [89,90]. Since drp1's function relies on large-scale structural rearrangements, the observed Imeglimin-induced conformational restriction suggests that Imeglimin may act as a negative modulator of drp1, thereby reducing excessive mitochondrial fragmentation. Imeglimin's modulation of drp1 may contribute to its mitochondrial protective effects.

Imeglimin-Hexokinase 2

Hexokinase 2 catalyzes the first step in glycolysis by catalyzing the phosphorylation of Glucose and is the key enzyme of this process. It also plays a crucial role in mitochondrial protection and autophagy. Hexokinase 2 binds to the Outer Mitochondrial membrane, coupling energy metabolism and cell survival [91]. The binding of Hexokinase 2 to OMM prevents the formation of mitochondrial permeability pore, thereby preventing apoptosis [92]. Hexokinase 2 has a linker, N-terminal (NTD) and C-terminal (CTD) domain, with the NTD and CTD having large and small subdomains [93].

The crystal structure of human hexokinase 2 (PDB ID: 2NZT) was used for computational analysis. Molecular docking study revealed that Imeglimin forms hydrogen bonds with Gly86, Gly87, Asn89, Phe90, Ile114, and Met119, with a strong hydrophobic interaction at Ile119. However, during MD simulations, a shift in the binding interactions was observed with persistent hydrogen bonding occurring at Lys337, Ser340, Ser415, Val416, and Lys419, and hydrophobic interaction was observed at Thr232, suggesting a binding site migration. All these residues are located in the N-terminal domain of Hexokinase 2 [94]. RMSF analysis indicated that the interacting residues Ser415 and Val416 exhibited lower fluctuations, suggesting stable ligand–protein interactions. Moderate flexibility in Lys337, Ser340, and Lys419 indicated localized conformational adaptability. The RMSD of the HK2-Imeglimin complex fluctuated between 1.2Å and 4.2 Å, indicating that Imeglimin does not rigidly stabilize HK2 but allows structural adaptability as observed by the occasional fluctuations. The Rg analysis confirms that the complex maintained its compactness without major structural expansion or collapse. PCA analysis revealed that PC1 and PC2 accounted for 60.3% of the total variance, indicating that Imeglimin influences Hexokinase 2's structural dynamics. The broad conformational space observed in PC projections suggests that HK2 retains flexibility rather than adopting a single rigid state; however, a shift to a more constrained cluster was noted over time, implying that Imeglimin-modulated HK2's motion while maintaining functional adaptability. The steep variance drop after PC2 further supports that major functional motions are primarily captured in the first two components. DCCM analysis showed strongly correlated motions within localized structures, while anti-correlated motions in distant residues indicating differential inter-domain flexibility. Binding-free energy calculations show that Imeglimin binds with HK2 with a moderate affinity, with contributions primarily from van der Waals interactions and solvation effects, while electrostatic interactions were destabilizing, suggesting that Imeglimin does not form highly stable interactions with HK2. The energetics and the binding-induced conformational adaptability observed in this study suggest that Imeglimin may influence Hexokinase 2's activity, but not significantly.

Imeglimin-NLRP3

NLRP3, belonging to the Signal transduction ATPases with numerous domains group of ATPases exists in an auto-inhibited state in the cytoplasm, wherein the NATCH domain remains in an inactive configuration and acts as a sensor to both infection-mediated and sterile inflammatory signals [95]. On activation, ATP binding causes a conformational shift leading to oligomerization and activation of the caspase 1 pathway, thereby catalyzing the production of mature interleukins such as IL-1beta and IL-18 [96-99]. NLRP3 has an N-terminal Pyrin effector domain (PYD), a C-terminal LRR domain, and a central NATCH domain, which in turn has 4 subdomains: the Nucleotide-binding domain, Helical Domain 1 (HD1), Winged helical domain, and HD2.

The crystal structure of NLRP3 (PDB ID: 7ALV) was used for computational analysis. Molecular docking and MD simulations revealed that Imeglimin formed persistent hydrogen bonds with NLRP3 at Ala228, Ile574, Arg578, Glu629, and Tyr632 and hydrophobic interactions at Tyr632. Imeglimin binds to key residues in the NATCH domain, specifically Ala228, Arg578, and Glu629, which are essential for ATP binding and hydrolysis, suggesting a possible interference in the conformational change required for NLRP3 activation. In addition, its interaction with Tyr632 in LRR domain implies a potential impact on inflammasome assembly. The residues Ala228, Arg578, and Glu629 are also the critical binding sites for MCC950, whose inhibitory function arises from stabilizing the NATCH domain and preventing ATP-driven activation of NLRP3 [100,101]. Residue-specific RMSF analysis revealed that Arg578 exhibited the lowest fluctuation of 0.478 Å, indicating strong stabilization, while Glu629 and Try632 showed higher RMSF values (~0.87–1.2 Å), suggesting retained flexibility in the LRR domain. The stabilization of Arg578 is significant as it is a crucial ATP-binding residue, and its restricted movement suggests a possible impaired ATPase activity, which is essential for NLRP3 activation [101]. The RMSD analysis showed that Imeglimin–NLRP3 complex exhibited early fluctuation during the simulations, reflecting initial structural adjustments. Beyond this phase, the RMSD stabilized around 1.2–1.3 Å from 20 ns onward, indicating that Imeglimin binding possibly restricts major structural transitions but allows limited local flexibility. The Rg remained stable ~23.1 Å, indicating that Imeglimin binding maintains NLRP3 in a compact state without inducing large-scale unfolding. This indicates that Imeglimin does not cause destabilization but instead possibly stabilizes a constrained conformation that may prevent the necessary flexibility required for full inflammasome activation. PCA analysis revealed that PC1 (39.47%) captures the dominant structural motion, primarily within the NATCH domain. PC2 (9.14%) and PC3 (6.15%) represent additional localized fluctuations, particularly within the LRR domain, suggesting that Imeglimin binding influences intra-domain interactions but does not induce full activation-related rearrangements. DCCM analysis further supported these findings, showing strong positive correlations within the NATCH domain, indicating Imeglimin stabilized intra-domain interactions. Anti-correlated motions between NATCH and LRR suggest localized flexibility in the LRR domain, aligning with the hypothesis that Imeglimin may restrict ATP-driven NATCH activation while allowing some conformational adaptability in the LRR domain. Binding-free energy calculation using MM/GBSA indicates that Imeglimin binds ti NLRP3 with moderate affinity of −12.9 kcal/mol, predominantly driven by strong electrostatic interactions (−126.0 kcal/mol) with additional Van der Waals stabilization (−15.87 kcal/mol). However, a high solvation penalty (+129.0 kcal/mol) reduces the overall binding strength. This structural modulation may prevent full NLRP3 activation and downstream inflammatory signaling, aligning with Imeglimin's known roles in metabolic and mitochondrial homeostasis.

Limitations

This study is based solely on *in silico* predictions and lacks experimental validation. The use of static crystal structures may not reflect full conformational flexibility under physiological conditions. Cellular complexity is not fully captured. Post-translational modifications such as phosphorylation or ubiquitination, which can affect binding, were not considered.

CONCLUSION

This *in silico* study systematically investigates the interaction of Imeglimin with five key proteins involved in mitochondrial function and cellular stress responses: AKT1, Hexokinase2, Parkin, DRP1, and NLRP3. Molecular docking and dynamics simulations revealed that Imeglimin forms stable and energetically favorable interactions with critical residues within the functional domains of each protein. In AKT1, Imeglimin binds within the kinase domain but outside the activation loop, suggesting a stabilizing influence that may affect phosphorylation dynamics. For Parkin, Imeglimin targets both regulatory and catalytic domains, potentially weakening intra-domain inhibition and promoting a primed state. In DRP1, binding within the GTPase domain, especially at Asn246 of G5 motif indicates restricted GTP binding and reduced fission dynamics. In NLRP3, interactions suggest that Imeglimin might prevent a full-scale activation of NLRP3. Hexokinase 2, by contrast, exhibited binding site migration and weaker interaction energies, indicating minimal structural influence. Collectively, these findings support the hypothesis that Imeglimin acts as a multi-target mitochondrial modulator, with strong effects seen in DRP1, Parkin, and NLRP3 proteins that are central to mitochondrial dynamics, autophagy, and immune signaling. This structural insight provides a mechanistic basis for Imeglimin's mitochondrial protective and immunomodulatory roles observed. Further experimental studies are needed to confirm and extend these findings.

CONFLICT OF INTEREST

The authors declare no conflict of interest.

ACKNOWLEDGMENT

The authors would like to express heartfelt gratitude to the Department of Pharmacology, SRMC, and RI.

FUNDING

Nil.

REFERENCES

1. Tait SW, Green DR. Mitochondria and cell signalling. J Cell Sci. 2012 Feb 15;125(4):807-15. doi: 10.1242/jcs.099234, PMID 22448037
2. López-Armada MJ, Riveiro-Naveira RR, Vaamonde-García C, Valcárcel-Ares MN. Mitochondrial dysfunction and the inflammatory response. Mitochondrion. 2013 Mar 1;13(2):106-18. doi: 10.1016/j.mito.2013.01.003, PMID 23333405
3. Bhatti JS, Bhatti GK, Reddy PH. Mitochondrial dysfunction and oxidative stress in metabolic disorders - a step towards mitochondria based therapeutic strategies. Biochim Biophys Acta Mol Basis Dis. 2017 May 1;1863(5):1066-77. doi: 10.1016/j.bbadis.2016.11.010, PMID 27836629
4. Turrens JF. Mitochondrial formation of reactive oxygen species. J Physiol. 2003 Oct 15;552(2):335-44. doi: 10.1113/jphysiol.2003.049478, PMID 14561818
5. Naik E, Dixit VM. Mitochondrial reactive oxygen species drive proinflammatory cytokine production. J Exp Med. 2011 Mar 14;208(3):417-20. doi: 10.1084/jem.20110367, PMID 21357740
6. Moodley D, Mody G, Patel N, Chuturgoon AA. Mitochondrial depolarisation and oxidative stress in rheumatoid arthritis patients. Clin Biochem. 2008 Nov;41(16-17):1396-401. doi: 10.1016/j.clinbiochem.2008.08.072, PMID 18789914
7. Harty LC, Biniecka M, O'Sullivan J, Fox E, Mulhall K, Veale DJ, *et al*. Mitochondrial mutagenesis correlates with the local inflammatory environment in arthritis. Ann Rheum Dis. 2012 Apr;71(4):582-8. doi: 10.1136/annrheumdis-2011-200245, PMID 22121133
8. Gergely P Jr., Grossman C, Niland B, Puskas F, Neupane H, Allam F, *et al*. Mitochondrial hyperpolarization and ATP depletion in patients with systemic lupus erythematosus. Arthritis Rheum. 2002;46(1):175-90. doi: 10.1002/1529-0131(200201)46:1<175:AID-ART10015>3.0.CO;2-H, PMID 11817589
9. Vaamonde-García C, Riveiro-Naveira RR, Valcárcel-Ares MN, Hermida-Carballo L, Blanco FJ, Lõpez-Armada MJ. Mitochondrial dysfunction increases inflammatory responsiveness to cytokines in normal human chondrocytes. Arthritis Rheum. 2012 Sep;64(9):2927-36. doi: 10.1002/art.34508, PMID 22549761
10. Yang J, Guo Q, Feng X, Liu Y, Zhou Y. Mitochondrial dysfunction in cardiovascular diseases: Potential targets for treatment. Front Cell Dev Biol. 2022 May 13;10:841523. doi: 10.3389/fcell.2022.841523, PMID 35646910
11. Killackey SA, Philpott DJ, Girardin SE. Mitophagy pathways in health and disease. J Cell Biol. 2020 Nov 2;219(11):e202004029. doi: 10.1083/jcb.202004029, PMID 32926082
12. Witte ME, Geurts JJ, De Vries HE, Van Der Valk P, Van Horssen J. Mitochondrial dysfunction: A potential link between neuroinflammation and neurodegeneration? Mitochondrion. 2010 Aug;10(5):411-8. doi: 10.1016/j.mito.2010.05.014, PMID 20573557
13. Pizarro-Galleguillos BM, Kunert L, Brüggemann N, Prasuhn J. Neuroinflammation and mitochondrial dysfunction in Parkinson's disease: connecting neuroimaging with pathophysiology. Antioxidants (Basel). 2023 Jul 12;12(7):1411. doi: 10.3390/antiox12071411, PMID 37507950
14. Di Filippo M, Chiasserini D, Tozzi A, Picconi B, Calabresi P. Mitochondria and the link between neuroinflammation and neurodegeneration. J Alzheimers Dis. 2010;20 Suppl 2:S369-79. doi: 10.3233/JAD-2010-100543, PMID 20463396
15. Mandemakers W, Morais VA, De Strooper B. A cell biological perspective on mitochondrial dysfunction in Parkinson disease and other neurodegenerative diseases. J Cell Sci. 2007 May 15;120(10):1707-16. doi: 10.1242/jcs.03443, PMID 17502481
16. Morán M, Moreno-Lastres D, Marín-Buera L, Arenas J, Martín MA, Ugalde C. Mitochondrial respiratory chain dysfunction: Implications in neurodegeneration. Free Radic Biol Med. 2012 Aug 1;53(3):595-609. doi: 10.1016/j.freeradbiomed.2012.05.009, PMID 22595027
17. Cozzolino M, Seli E. Mitochondrial function in women with polycystic ovary syndrome. Curr Opin Obstet Gynecol. 2020 Jun 1;32(3):205-12. doi: 10.1097/GCO.0000000000000619, PMID 32068544
18. Sangwung P, Petersen KF, Shulman GI, Knowles JW. Potential role of alterations in mitochondrial function in the pathogenesis of insulin resistance and type 2 diabetes. Endocrinology (US). 2021;161(4):1-10.
19. Das M, Sauceda C, Webster NJ. Mitochondrial dysfunction in obesity and reproduction. Endocrinology. 2021 Jan 1;162(1):bqaa158. doi: 10.1210/endocr/bqaa158, PMID 32945868
20. Hebert JF, Myatt L. Placental mitochondrial dysfunction with metabolic diseases: Therapeutic approaches. Biochim Biophys Acta Mol Basis Dis. 2021 Jan 1;1867(1):165967. doi: 10.1016/j.bbadis.2020.165967, PMID 32920120
21. Kasapoğlu I, Seli E. Mitochondrial dysfunction and ovarian aging. Endocrinology. 2020 Feb 1;161(2):bqaa001. doi: 10.1210/endocr/bqaa001, PMID 31927571
22. Moore MP, Cunningham RP, Meers GM, Johnson SA, Wheeler AA, Ganga RR, *et al*. Compromised hepatic mitochondrial fatty acid oxidation and reduced markers of mitochondrial turnover in human NAFLD. Hepatology. 2022 Nov 1;76(5):1452-65. doi: 10.1002/hep.32324, PMID 35000203
23. Chen P, Yao L, Yuan M, Wang Z, Zhang Q, Jiang Y, *et al*. Mitochondrial dysfunction: A promising therapeutic target for liver diseases. Genes Dis. 2024 May 1;11(3):101115. doi: 10.1016/j.gendis.2023.101115, PMID 38299199
24. Chiu HY, Tay EX, Ong DS, Taneja R. Mitochondrial dysfunction at the center of cancer therapy. Antioxid Redox Signal. 2020 Jan 8;32(5):309-30. doi: 10.1089/ars.2019.7898, PMID 31578870
25. Boland ML, Chourasia AH, Macleod KF. Mitochondrial dysfunction in cancer. Front Oncol. 2013;3:292. doi: 10.3389/fonc.2013.00292, PMID 24350057
26. Guerra F, Guaragnella N, Arbini AA, Bucci C, Giannattasio S, Moro L. Mitochondrial dysfunction: A novel potential driver of epithelial-to-mesenchymal transition in cancer. Front Oncol. 2017 Dec 1;7:295. doi: 10.3389/fonc.2017.00295, PMID 29250487
27. Zeviani M, Di Donato S. Mitochondrial disorders. Brain. 2004 Oct 1;127(10):2153-72. doi: 10.1093/brain/awh259, PMID 15358637

28. Niyazov DM, Kahler SG, Frye RE. Primary mitochondrial disease and secondary mitochondrial dysfunction: Importance of distinction for diagnosis and treatment. Mol Syndromol. 2016 Jul 1;7(3):122-37. doi: 10.1159/000446586, PMID 27587988
29. Grel H, Woznica D, Ratajczak K, Kalwarczyk E, Anchimowicz J, Switlik W, *et al*. Mitochondrial dynamics in neurodegenerative diseases: Unraveling the role of fusion and fission processes. Int J Mol Sci. 2023 Aug 22;24(17):13033. doi: 10.3390/ijms241713033, PMID 37685840
30. Archer SL. Mitochondrial dynamics--mitochondrial fission and fusion in human diseases. N Engl J Med. 2013 Dec 5;369(23):2236-51. doi: 10.1056/NEJMra1215233, PMID 24304053
31. Valero T. Mitochondrial biogenesis: Pharmacological approaches. Curr Pharm Des. 2014 Sep 15;20(35):5507-9. doi: 10.2174/1381612820351 40911142118, PMID 24606795
32. Singh A, Faccenda D, Campanella M. Pharmacological advances in mitochondrial therapy. EBioMedicine. 2021 Mar 1;65:103244. doi: 10.1016/j.ebiom.2021.103244, PMID 33647769
33. Rahman MM, Tumpa MA, Rahaman MS, Islam F, Sutradhar PR, Ahmed M, *et al*. Emerging promise of therapeutic approaches targeting mitochondria in neurodegenerative disorders. Curr Neuropharmacol. 2023 Mar 17;21(5):1081-99. doi: 10.2174/1570159X21666230316150 559, PMID 36927428
34. Mangrulkar SV, Wankhede NL, Kale MB, Upaganlawar AB, Taksande BG, Umekar MJ, *et al*. Mitochondrial dysfunction as a signaling target for therapeutic intervention in major neurodegenerative disease. Neurotox Res. 2023 Dec 1;41(6):708-29. doi: 10.1007/s12640-023-00647-2, PMID 37162686
35. Brown DA, Perry JB, Allen ME, Sabbah HN, Stauffer BL, Shaikh SR, *et al*. Mitochondrial function as a therapeutic target in heart failure. Nat Rev Cardiol. 2016;14(4):238-250.
36. Murphy MP, Hartley RC. Mitochondria as a therapeutic target for common pathologies. Nat Rev Drug Discov. 2018 Nov 28;17(12):865-86. doi: 10.1038/nrd.2018.174, PMID 30393373
37. Konkwo C, Perry RJ. Imeglimin: Current development and future potential in type 2 diabetes. Drugs. 2021 Feb 1;81(2):185-90. doi: 10.1007/s40265-020-01434-5, PMID 33247829
38. Yaribeygi H, Maleki M, Sathyapalan T, Jamialahmadi T, Sahebkar A. Molecular mechanisms by which imeglimin improves glucose homeostasis. J Diabetes Res. 2020;2020:8768954. doi: 10.1155/2020/8768954, PMID 32215274
39. Detaille D, Vial G, Borel AL, Cottet-Rouselle C, Hallakou-Bozec S, Bolze S, *et al*. Imeglimin prevents human endothelial cell death by inhibiting mitochondrial permeability transition without inhibiting mitochondrial respiration. Cell Death Discov. 2016;2(1):15072. doi: 10.1038/cddiscovery.2015.72, PMID 27551496
40. Sanada J, Obata A, Fushimi Y, Kimura T, Shimoda M, Ikeda T, *et al*. Imeglimin exerts favorable effects on pancreatic β-cells by improving morphology in mitochondria and increasing the number of insulin granules. Sci Rep. 2022;12(1):13220. doi: 10.1038/s41598-022-17657-3, PMID 35918386
41. Zemgulyte G, Umbrasas D, Cizas P, Jankeviciute S, Pampuscenko K, Grigaleviciute R, *et al*. Imeglimin is neuroprotective against ischemic brain injury in rats- a study evaluating neuroinflammation and mitochondrial functions. Mol Neurobiol. 2022 May 1;59(5):2977-91. doi: 10.1007/s12035-022-02765-y, PMID 35257284
42. Lee JY, Kang Y, Jeon JY, Kim HJ, Kim DJ, Lee KW, *et al*. Imeglimin attenuates NLRP3 inflammasome activation by restoring mitochondrial functions in macrophages. J Pharmacol Sci. 2024 Jun 1;155(2):35-43. doi: 10.1016/j.jphs.2024.03.004, PMID 38677784
43. Kato H, Iwashita K, Iwasa M, Kato S, Yamakage H, Suganami T, *et al*. Imeglimin exhibits novel anti-inflammatory effects on high-glucose-stimulated mouse microglia through ULK1-mediated suppression of the TXNIP-NLRP3 axis. Cells. 2024 Feb 1;13(3):284. doi: 10.3390/cells13030284, PMID 38334676
44. RCSB PDB - 7NH5: Co-crystal structure of Akt1. In: Complex Covalent-Allosteric Akt Inhibitor. Vol. 6. California: RCSB; 2021 Sep 08. Available from: https://www.rcsb.org/structure/7NH5 [Last accessed on 2025 Feb 12].
45. Crystal Structure of Human Dlp1 in Complex with GDP; 2014 Feb 19. p. AlF4. Available from: https://www.wwpdb.org/pdb?id=pdb_00003w6p [Last accessed on 2025 Feb 12].
46. RCSB PDB - 5C1Z: Parkin (UblR0RBR). Available from: https://www.rcsb.org/structure/5C1Z [Last accessed on 2025 Feb 12].
47. Crystal Structure of NLRP3 NACHT Domain in Complex with a Potent Inhibitor; 2021 Oct 20. Available from: https://www.wwpdb.org/pdb?id=pdb_00007alv [Last accessed on 2025 Feb 12].
48. RCSB PDB - 2NZT: Crystal Structure of Human Hexokinase. Vol. 2. Available from: https://www.rcsb.org/structure/2NZT [Last accessed on 2025 Feb 12].
49. Tian C, Kasavajhala K, Belfon KA, Raguette L, Huang H, Migues AN, *et al*. Ff19SB: Amino-acid-specific protein backbone parameters trained against quantum mechanics energy surfaces in solution. J Chem Theor Comput. 2020 Jan 14;16(1):528-52. doi: 10.1021/acs.jctc.9b00591, PMID 31714766
50. Case DA, Aktulga HM, Belfon K, Cerutti DS, Cisneros GA, Cruzeiro VW, *et al*. AmberTools. J Chem Inf Model. 2023 Oct 23;63(20):6183-91. doi: 10.1021/acs.jcim.3c01153, PMID 37805934
51. Eastman P, Swails J, Chodera JD, McGibbon RT, Zhao Y, Beauchamp KA, *et al*. OpenMM 7: Rapid development of high performance algorithms for molecular dynamics. PLOS Comput Biol. 2017 Jul 1;13(7):e1005659. doi: 10.1371/journal.pcbi.1005659, PMID 28746339
52. Roe DR, Cheatham TE 3rd. PTRAJ and CPPTRAJ: Software for processing and analysis of molecular dynamics trajectory data. J Chem Theor Comput. 2013 Jul 9;9(7):3084-95. doi: 10.1021/ct400341p, PMID 26583988
53. Truebestein L, Hornegger H, Anrather D, Hartl M, Fleming KD, Stariha JT, *et al*. Structure of autoinhibited Akt1 reveals mechanism of PIP3-mediated activation. Proc Natl Acad Sci U S A. 2021 Aug 17;118(33):e2101496118. doi: 10.1073/pnas.2101496118, PMID 34385319
54. Pearce LR, Komander D, Alessi DR. The nuts and bolts of AGC protein kinases. Nat Rev Mol Cell Biol. 2010;11(1):9-22. doi: 10.1038/nrm2822, PMID 20027184
55. Heron-Milhavet L, Khouya N, Fernandez A, Lamb NJ. Akt1 and Akt2: Differentiating the action. Histol Histopathol. 2011 May;26(5):651-62. doi: 10.14670/HH-26.651, PMID 21432781
56. Häggblad Sahlberg SH, Mortensen AC, Haglöf J, Engskog MK, Arvidsson T, Pettersson C, *et al*. Different functions of AKT1 and AKT2 in molecular pathways, cell migration and metabolism in colon cancer cells. Int J Oncol. 2017 Jan 1;50(1):5-14. doi: 10.3892/ijo.2016.3771, PMID 27878243
57. Duggal S, Jailkhani N, Midha MK, Agrawal N, Rao KV, Kumar A. Defining the Akt1 interactome and its role in regulating the cell cycle. Sci Rep. 2018 Dec 1;8(1):1303. doi: 10.1038/s41598-018-19689-0, PMID 29358593
58. Guerau-De-Arellano M, Piedra-Quintero ZL, Tsichlis PN. Akt isoforms in the immune system. Front Immunol. 2022 Aug 23;13:990874. doi: 10.3389/fimmu.2022.990874, PMID 36081513
59. Datta SR, Brunet A, Greenberg ME. Cellular survival: A play in three Akts. Genes Dev. 1999;13(22):2905-27. doi: 10.1101/gad.13.22.2905, PMID 10579998
60. Liao Y, Hung MC. Physiological regulation of Akt activity and stability. Am J Transl Res. 2010;2(1):19-42. PMID 20182580
61. Bos JL. A target for phosphoinositide 3-kinase: Akt/PKB. Trends Biochem Sci. 1995;20(11):441-2. doi: 10.1016/s0968-0004(00)89097-0, PMID 8578585
62. Hanada M, Feng J, Hemmings BA. Structure, regulation and function of PKB/AKT--a major therapeutic target. Biochim Biophys Acta. 2004 Mar 11;1697(1-2):3-16. doi: 10.1016/j.bbapap.2003.11.009, PMID 15023346
63. Lučic I, Rathinaswamy MK, Truebestein L, Hamelin DJ, Burke JE, Leonard TA. Conformational sampling of membranes by Akt controls its activation and inactivation. Proc Natl Acad Sci U S A. 2018 Apr 24;115(17):E3940-9. doi: 10.1073/pnas.1716109115, PMID 29632185
64. Xie X, Shu R, Yu C, Fu Z, Li Z. Mammalian AKT, the emerging roles on mitochondrial function in diseases. Aging Dis. 2022 Feb 1;13(1):157-74. doi: 10.14336/AD.2021.0729, PMID 35111368
65. Parcellier A, Tintignac LA, Zhuravleva E, Hemmings BA. PKB and the mitochondria: AKTing on apoptosis. Cell Signal. 2008 Jan;20(1):21-30. doi: 10.1016/j.cellsig.2007.07.010, PMID 17716864
66. Guha M, Fang JK, Monks R, Birnbaum MJ, Avadhani NG. Activation of Akt is essential for the propagation of mitochondrial respiratory stress signaling and activation of the transcriptional coactivator heterogeneous ribonucleoprotein A2. Mol Biol Cell. 2010 Oct 15;21(20):3578-89. doi: 10.1091/mbc.E10-03-0192, PMID 20719961
67. Cantrell D. Protein kinase B (Akt) regulation and function in T lymphocytes. Semin Immunol. 2002;14(1):19-26. doi: 10.1006/smim.2001.0338, PMID 11884227
68. Vergadi E, Ieronymaki E, Lyroni K, Vaporidi K, Tsatsanis C. Akt signaling pathway in macrophage activation and M1/M2

polarization. J Immunol. 2017 Feb 1;198(3):1006-14. doi: 10.4049/jimmunol.1601515, PMID 28115590
69. Takahashi N, Kimura AP, Yoshizaki T, Ohmura K. Imeglimin modulates mitochondria biology and facilitates mitokine secretion in 3T3-L1 adipocytes. Life Sci. 2024 Jul 15;349:122735. doi: 10.1016/j.lfs.2024.122735, PMID 38768776
70. Gundogdu M, Tadayon R, Salzano G, Shaw GS, Walden H. A mechanistic review of Parkin activation. Biochim Biophys Acta Gen Subj. 2021 Jun 1;1865(6):129894. doi: 10.1016/j.bbagen.2021.129894, PMID 33753174
71. Koyano F, Matsuda N. Molecular mechanisms underlying PINK1 and Parkin catalyzed ubiquitylation of substrates on damaged mitochondria. Biochim Biophys Acta Mol Cell Res. 2015 Oct 1;1853;10:2791-6.
72. Wauer T, Komander D. Structure of the human Parkin ligase domain in an autoinhibited State. EMBO J. 2013 Jul 31;32(15):2099-112. doi: 10.1038/emboj.2013.125, PMID 23727886
73. Chaugule VK, Burchell L, Barber KR, Sidhu A, Leslie SJ, Shaw GS, *et al*. Autoregulation of Parkin activity through its ubiquitin-like domain. EMBO J. 2011 Jul 20;30(14):2853-67. doi: 10.1038/emboj.2011.204, PMID 21694720
74. Trempe JF, Sauvé V, Grenier K, Seirafi M, Tang MY, Meńade M, *et al*. Structure of parkin reveals mechanisms for ubiquitin ligase activation. Science. 2013 Jun 21;340(6139):1451-5.
75. Islam NN, Weber CA, Coban M, Cocker LT, Fiesel FC, Springer W, *et al*. *In silico* investigation of parkin-activating mutations using simulations and network modeling. Biomolecules. 2024 Mar 1;14(3):365. doi: 10.3390/biom14030365, PMID 38540783
76. Kumar A, Aguirre JD, Condos TE, Martinez-Torres RJ, Chaugule VK, Toth R, *et al*. Disruption of the autoinhibited state primes the E3 ligase Parkin for activation and catalysis. EMBO J. 2015 Oct 14;34(20):2506-21. doi: 10.15252/embj.201592337, PMID 26254304
77. Dove KK, Klevit RE, Rittinger K. pUBLically unzipping Parkin: How phosphorylation exposes a ligase bit by bit. EMBO J. 2015 Oct 14;34(20):2486-8. doi: 10.15252/embj.201592857, PMID 26346274
78. Wasner K, Smajic S, Ghelfi J, Delcambre S, Prada-Medina CA, Knappe E, *et al*. Parkin deficiency impairs mitochondrial DNA dynamics and propagates inflammation. Mov Disord. 2022 Jul 1;37(7):1405-15. doi: 10.1002/mds.29025, PMID 35460111
79. Frank-Cannon TC, Tran T, Ruhn KA, Martinez TN, Hong J, Marvin M, *et al*. Parkin deficiency increases vulnerability to inflammation-related nigral degeneration. J Neurosci. 2008 Oct 22;28(43):10825-34. doi: 10.1523/JNEUROSCI.3001-08.2008, PMID 18945890
80. Henn IH, Bouman L, Schlehe JS, Schlierf A, Schramm JE, Wegener E, *et al*. Parkin mediates neuroprotection through activation of IkappaB kinase/nuclear factor-kappa B signaling. J Neurosci. 2007 Feb 21;27(8):1868-78. doi: 10.1523/JNEUROSCI.5537-06.2007, PMID 17314283
81. Amadoro G, Corsetti V, Florenzano F, Atlante A, Bobba A, Nicolin V, *et al*. Morphological and bioenergetic demands underlying the mitophagy in post-mitotic neurons: The pink-parkin pathway. Front Aging Neurosci. 2014;6:18. doi: 10.3389/fnagi.2014.00018, PMID 24600391
82. Grenier K, McLelland GL, Fon EA. Parkin- and PINK1-dependent mitophagy in neurons: Will the real pathway please stand up? Front Neurol. 2013;4:100. doi: 10.3389/fneur.2013.00100, PMID 23882257
83. Ge P, Dawson VL, Dawson TM. PINK1 and Parkin mitochondrial quality control: A source of regional vulnerability in Parkinson's disease. Mol Neurodegener. 2020;15(1):20. doi: 10.1186/s13024-020-00367-7, PMID 32169097
84. Vial G, Chauvin MA, Bendridi N, Durand A, Meugnier E, Madec AM, *et al*. Imeglimin normalizes glucose tolerance and insulin sensitivity and improves mitochondrial function in liver of a high-fat, high-sucrose diet mice model. Diabetes. 2015 Jun 1;64(6):2254-64. doi: 10.2337/db14-1220, PMID 25552598
85. Ji WK, Hatch AL, Merrill RA, Strack S, Higgs HN. Actin filaments target the oligomeric maturation of the dynamin GTpase Drp1 to mitochondrial fission sites. eLife. 2015 Nov 26;4:e11553. doi: 10.7554/eLife.11553, PMID 26609810
86. Wenger J, Klinglmayr E, Fröhlich C, Eibl C, Gimeno A, Hessenberger M, *et al*. Functional mapping of human Dynamin-1-Like GTPase domain based on X-ray structure analyses. PLOS One. 2013;8(8):e71835. doi: 10.1371/journal.pone.0071835, PMID 23977156
87. Faelber K, Held M, Gao S, Posor Y, Haucke V, Noé F, *et al*. Structural insights into dynamin-mediated membrane fission. Structure. 2012 Oct 10;20(10):1621-8. doi: 10.1016/j.str.2012.08.028, PMID 23063009
88. Otera H, Ishihara N, Mihara K. New insights into the function and regulation of mitochondrial fission. Biochim Biophys Acta Mol Cell Res. 2013 May;1833(5):1256-68. doi: 10.1016/j.bbamcr.2013.02.002
89. Wu D, Dasgupta A, Chen KH, Neuber-Hess M, Patel J, Hurst TE, *et al*. Identification of novel dynamin-related protein 1 (Drp1) GTPase inhibitors: Therapeutic potential of Drpitor1 and Drpitor1a in cancer and cardiac ischemia-reperfusion injury. FASEB J. 2020 Jan 1;34(1):1447-64. doi: 10.1096/fj.201901467R, PMID 31914641
90. Ruiz A, Alberdi E, Matute C. Mitochondrial division inhibitor 1 (Mdivi-1) protects neurons against excitotoxicity through the modulation of mitochondrial function and intracellular Ca2+ signaling. Front Mol Neurosci. 2018 Jan 17;11:3. doi: 10.3389/fnmol.2018.00003, PMID 29386996
91. Roberts DJ, Miyamoto S. Hexokinase II integrates energy metabolism and cellular protection: Akting on mitochondria and TORCing to autophagy. Cell Death Differ. 2014;22(2):248-57.
92. Botzer LE, Maman S, Sagi-Assif O, Meshel T, Nevo I, Yron I, *et al*. Hexokinase 2 is a determinant of neuroblastoma metastasis. Br J Cancer. 2016 Mar 1;114(7):759-66. doi: 10.1038/bjc.2016.26, PMID 26986252
93. Ferreira JC, Khrbtli AR, Shetler CL, Mansoor S, Ali L, Sensoy O, *et al*. Linker residues regulate the activity and stability of hexokinase 2, a promising anticancer target. J Biol Chem. 2020 Jan 1;296:100071.
94. HK1 - Hexokinase-2 - Homo sapiens (Human). UniProtKB. UniProt. Available from: https://www.uniprot.org/uniprotkb/a0A994J758/entry [Last accessed on 2025 Mar 04].
95. Brinkschulte R, Fußhöller DM, Hoss F, Rodríguez-Alcázar JF, Lauterbach MA, Kolbe CC, *et al*. ATP-binding and hydrolysis of human NLRP3. Commun Biol. 2022;5(1):1176. doi: 10.1038/s42003-022-04120-2, PMID 36329210
96. Fu J, Wu H. Structural mechanisms of NLRP3 inflammasome assembly and activation. Annu Rev Immunol. 2023 Apr 26;41:301-16. doi: 10.1146/annurev-immunol-081022-021207, PMID 36750315
97. Dekker C, Mattes H, Wright M, Boettcher A, Hinniger A, Hughes N, *et al*. Crystal structure of NLRP3 NACHT domain with an inhibitor defines mechanism of inflammasome inhibition. J Mol Biol. 2021 Dec 3;433(24):167309. doi: 10.1016/j.jmb.2021.167309, PMID 34687713
98. Jin C, Flavell RA. Molecular mechanism of NLRP3 inflammasome activation. J Clin Immunol. 2010 Sep 30;30(5):628-31. doi: 10.1007/s10875-010-9440-3, PMID 20589420
99. Ma Q. Pharmacological inhibition of the NLRP3 inflammasome: Structure, molecular activation, and inhibitor-NLRP3 interaction. Pharmacol Rev. 2023 May 1;75(3):487-520. doi: 10.1124/pharmrev.122.000629, PMID 36669831
100. Tapia-Abellán A, Angosto-Bazarra D, Martínez-Banaclocha H, De Torre-Minguela C, Cerón-Carrasco JP, Pérez-Sánchez H, *et al*. MCC950 closes the active conformation of NLRP3 to an inactive state. Nat Chem Biol. 2019 Jun 1;15(6):560-4. doi: 10.1038/s41589-019-0278-6, PMID 31086329
101. Dos Santos Nascimento IJ, De Aquino TM, Da Silva-Júnior EF. Molecular docking and dynamics simulation studies of a dataset of NLRP3 inflammasome inhibitors. Recent Adv Inflamm Allergy Drug Discov. 2021;15(2):80-6.